

- (11) Reynolds, N. M.; Savage, J. D.; Hsu, S. L. *Macromolecules* **1989**, *22*, 2867.
- (12) Painter, P. C.; Koenig, J. L. *J. Polym. Sci., Polym. Phys. Ed.* **1977**, *15*, 1885.
- (13) Snyder, R. W.; Painter, P. C. *Polymer* **1981**, *22*, 1633.
- (14) Liang, C. Y.; Krimm, S. *J. Polym. Sci.* **1958**, *27*, 241.
- (15) Jasse, B.; Monnerie, L. *J. Mol. Struct.* **1977**, *39*, 165.
- (16) Pulay, P.; Fogarasi, G.; Boggs, J. E. *J. Chem. Phys.* **1981**, *74*, 3999.
- (17) Kim, P. K.; Hsu, S. L.; Ishida, H. *Macromolecules* **1985**, *18*, 1905.
- (18) Kim, P. K.; Chang, C.; Hsu, S. L. *Polymer* **1986**, *27*, 34.
- (19) Zachariades, A. E.; Mead, W. T.; Porter, R. S. *Chem. Rev.* **1980**, *80*, 351.
- (20) Yoon, D. Y.; Sundararajan, P. R.; Flory, P. J. *Macromolecules* **1975**, *8*, 776.
- (21) Doherty, D. C.; Hopfinger, A. J. *Macromolecules* **1989**, *22*, 2472.
- (22) Wilson, E. B., Jr.; Decius, J. C.; Cross, P. G. *Molecular Vibrations: The Theory of Infrared and Raman Vibrational Spectra*; Dover: New York, 1980; p 325.
- (23) Schlotter, N. E.; Rabolt, J. F. *Polymer* **1984**, *25*, 165.
- (24) Snyder, R. G.; Schachtschneider, H. H. *Spectrochim. Acta* **1965**, *21*, 169.
- (25) La Lau, C.; Snyder, R. G. *Spectrochim. Acta* **1971**, *27A*, 2073.
- (26) Schachtschneider, H. H.; Snyder, R. G. *Spectrochim. Acta* **1963**, *19*, 117.
- (27) Peterlin, A. *Colloid Polym. Sci.* **1987**, *265*, 357.
- (28) Samuels, R. J. *J. Polym. Sci., Polym. Phys. Ed.* **1979**, *17*, 535.
- (29) Kaufmann, W.; Petermann, J.; Reynolds, N.; Thomas, E. L.; Hsu, S. L. *Polymer*, in press.
- (30) Snyder, R. G.; Schachtschneider, J. H. *Spectrochim. Acta* **1963**, *19*, 85.

Registry No. sPS, 28325-75-9.

Diffusion in Quasi Two-Dimensional Macromolecular Solutions

P. Eggl,[†] D. Pink,^{*†} B. Quinn,[†] H. Ringsdorf,[§] and E. Sackmann[†]

Theoretical Physics Institute, St. Francis Xavier University, Antigonish, Nova Scotia, Canada B2G 1C0, Physik Department, Biophysik Group, Technische Universität, München, D-8046, Garching, FRG, and Institut für Organische Chemie, Universität Mainz, Mainz, D-6500, FRG

Received May 1, 1989; Revised Manuscript Received December 13, 1989

ABSTRACT: Membranes composed of a linearly polymerized amphiphile (with molecules interconnected via functional groups attached to the head groups via spacers) and dimyristoylphosphatidylcholine (DMPC) were studied in order to test their usefulness as models of two-dimensional macromolecular solutions. For that purpose a comparative experimental and Monte Carlo simulation study of the lateral diffusion of monomeric tracers and the self-diffusion of macrolipids was performed. Measurements of the diffusion coefficients were performed by the photobleaching technique in giant vesicles and in asymmetric bilayers supported on argon-sputtered glass substrates, with the inner (proximal) monolayer being composed of DMPC and the outer (distal) of the macromolecular solution. In the former case polymerization was performed by UV (285-nm) excitation and carried out chemically in the latter by using a hydrophilic initiator. The hydrodynamic radii of the photochemically and chemically polymerized macrolipids were obtained from the self-diffusion coefficients (of the macrolipids) by the application of a recent theory of diffusion in membranes in frictional contact with solid surfaces. The friction is transmitted by a thin lubricating water film (of some 10-Å thickness) between the proximal monolayer and the solid surface and can lead to a strong dependence of the diffusion coefficient on the size of the diffusant. We found a ratio of the radii of the macrolipid (a_p) to the monomer (a_m) of $a_p/a_m \approx 7$ for the photochemically polymerized species and of $a_p/a_m \approx 70$ for the chemically polymerized species. By assuming that the 2D mean-square radius of gyration scales as $N^{3/4}$, we obtained a degree of polymerization of $N = 20$ for the former and of $N = 300$ for the latter case showing that chemical polymerization is essential for the preparation of large macrolipids. Monte Carlo simulations in order to calculate the diffusion coefficients of monomeric tracers and macrolipids were carried out for fractions of area covered by the macromolecules varying from 10% to 80%. Two polymer conformations, representing extreme cases, were considered: a collapsed two-dimensional coil and an extended chain. The best agreement was found to be between experimental and simulated diffusion coefficients obtained for a linear combination of the collapsed and extended chain models, with the probability of the polymers to be in their collapsed states being about 0.4. The comparison suggests a value of $N \approx 24$ for the degree of polymerization of the photochemically polymerized species in good agreement with the experimental value.

I. Introduction

Membranes composed of monomeric lipids and polymerized amphiphiles (called macrolipids in this paper) are becoming of great interest. Some examples of their practical applications are (1) the development of drug delivery systems,¹ (2) the stabilization of Langmuir-

Blodgett films, and (3) the mimicking (simulation) of cell surfaces.^{1b,2} In addition, polymerized membranes offer new possibilities to prepare low-dimensionality macromolecular solutions or gels in order to study their fundamental properties, such as scaling laws, configurations, and polymerization processes in two dimensions.

In the present work we report combined experimental and Monte Carlo simulation studies of the lateral diffusion of monomolecular and macromolecular species in quasi two-dimensional solutions of (linear) macromolecular lip-

[†] St. Francis Xavier University.

[‡] Technische Universität.

[§] Universität Mainz.

ids in free and supported lipid lamellae of dimyristoylphosphatidylcholine (DMPC).

Most measurements of the diffusion coefficients were performed in giant vesicles by the fluorescence recovery after a photobleaching (FRAP) technique. In one experiment we compared the diffusion coefficients of fluorescent-labeled monomeric and polymerized tracers in an asymmetric bilayer deposited on a glass substrate, with the bottom (proximal) monolayer being composed of DMPC and the upper (distal) of a macromolecular solution. By making use of a recent theory of diffusion in supported bilayers,³ we determined approximate values of the hydrodynamic radii of the macrolipids prepared by both photochemical and chemical polymerization.

The intention of the theoretical work is to estimate (a) the average size of the polymers and (b) the range of conformations that the polymers are sampling. Rather than try to model the polymer formation itself, we consider it more reliable to assume an average length and calculate diffusion coefficients for monomeric and polymerized tracers. We use some of the experimental results to obtain an estimate for the average length, and we then calculate the dependence of the diffusion coefficients upon the area fraction of the membrane covered by the macromolecules (the coverage). Rather than attempt to distinguish between a number of model systems with various conformational weights, we chose to study two extreme cases, which have the advantage that we thereby eliminate all internal conformational states. This approximation is acceptable in that we are not concerned with the possibility of phase separation, since we are using a sufficiently high temperature. Such entropic contributions to a free energy are therefore irrelevant. Accordingly, in the Monte Carlo simulation study two fixed polymer conformations representing two extreme cases were considered: a collapsed two-dimensional (disklike) coil (CP) and an extended (linear) rigid conformation (EP). These extreme cases are not as unrealistic as they appear when one considers the constraints imposed upon the conformations of the polymers because of bonding via the polar group (below). The diffusion coefficients of macromolecular and monomeric tracers were determined as a function of the area fraction of the membrane covered by the macromolecules (the coverage) and for 3 degrees of polymerization.

The phase diagram of the two-dimensional macromolecular solution was determined partially by static light scattering, and we present these results.

II. Materials and Experimental Methods

(i) Materials. Dimyristoylphosphatidylcholine (DMPC) was a commercial product (Fluka). The polymerizable amphiphiles were synthesized in the laboratory of H.R.

The amphiphile **1a** (abbreviated as 4,16-POMECY in the following^{2a}) carries one functional group attached to the head group of the amphiphile via a spacer and thus forms linear macrolipids. As a monomeric fluorescence label we used either 3,3'-diiodododecylcarbocyanine (abbreviated as diO-C₁₈) or dipalmitoylphosphatidylethanolamine labeled with NBD (7-nitro-2,1,3-benzoxadiazol-4-yl), which is abbreviated as NBD-DPPE. Macromolecular fluorescent probes were made by the addition of 1–2% of the amphiphile **1b**.

By the use of molecular models one can see that the polymers formed could be either collapsed objects or extended objects with relatively few internal degrees of freedom. This is the justification for the use of the two extreme polymer models (CP and EP) used.

(ii) Vesicle Preparation. Giant vesicles (cf. Figure 1) were prepared as follows: A thin film of the lipid was deposited onto a carefully cleaned microscope slide by solvent evaporation. For that purpose a small droplet (20 μ L) of a solution of the (mono-

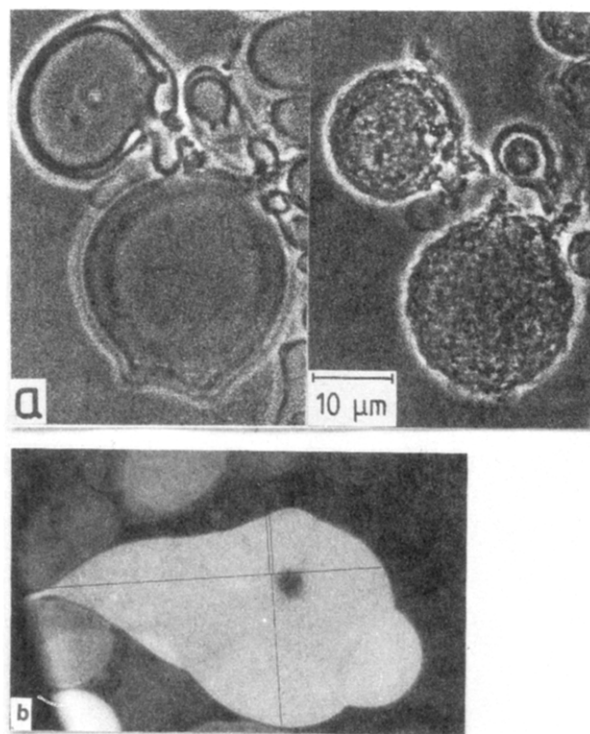
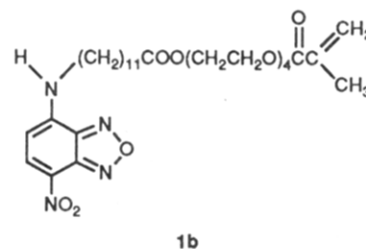
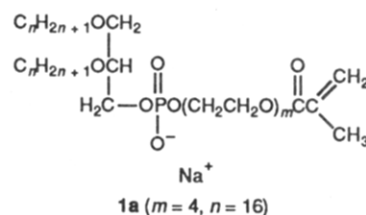


Figure 1. (a) Fluorescence micrograph of a giant vesicle of an equimolar mixture of DMPC and 4,16-POMECY (cf. the Materials section for abbreviations used). Note that some of the vesicles exhibit a very weak fluorescence, showing that they are thin walled and very likely single walled. The black spot (diameter 9 μ m) was produced by photobleaching some 5 s before the micrograph was taken. (b) Phase contrast photomicrograph of a vesicle containing a 1:1 mixture of DMPC and 4,16-POMECY showing the change of vesicle shape from quasispherical (left) to a cauliflower-like appearance (right), which is caused by photopolymerization for 4 min.



meric) lipids (7 mg/mL) in chloroform was deposited and the solvent was removed by evaporation in vacuo. A total of 200 μ L of Millipore water or buffer was then deposited on the microslide, which was then covered by a cover glass in such a way that no air bubbles were formed. In order to prevent solvent evaporation, the gap between the substrate and the cover glass was sealed by silicone grease. In order to swell the lipid, the sample was heated to 40 $^{\circ}$ C, which was well above the transition temperatures of both lipids (23 $^{\circ}$ C for DMPC and 29 $^{\circ}$ C for 4,16-POMECY). The sample was kept at this temperature for about 2 h. Very large vesicles formed during this time, some of which were very thin-walled; viz., two to three bilayers were seen in separate freeze-fracture electron microscopic studies.

(iii) Supported Bilayers. Symmetric bilayers were deposited onto microscope slides by the usual monolayer transfer

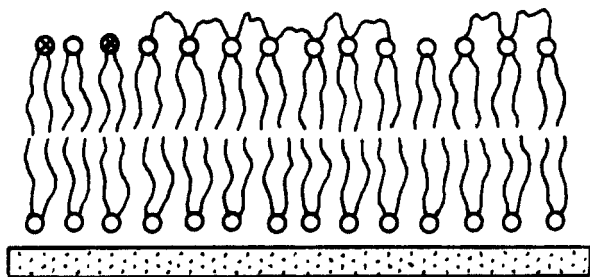


Figure 2. Schematic view of an asymmetric bilayer supported on a glass substrate. The latter is treated by argon sputtering in order to separate the monolayer closest to the substrate (called proximal) by a thin lubricating water film of some nanometer thickness.⁵

technique,⁴ and the procedure has been described in detail.⁵ For the present work the monolayer closest to the substrate (called the proximal layer in what follows) was DMPC while the outermost (distal) monolayer was a mixture of DMPC with monomeric or polymerized 4,16-POMEYC. In order to decouple the proximal monolayer from the substrate by a thin (some 10 Å thick) water film, the glass was sputtered by argon in a microwave discharge (Figure 2).⁵ The pressure of the film balance at which the transfer occurred was kept at a value where the monolayers are in a fluid state.

(iv) Polymerization Procedures. The photochemical polymerization of the giant vesicles was accomplished by irradiation with a low-pressure mercury UV lamp at maximum intensity at 254 nm wavelength (Penray Lamp Oriel Nr. 6035). For that purpose the flat cell was briefly removed from the microscope and held at a distance of 4 cm from the lamp for 4 min. In order to avoid photodecomposition, light of a wavelength shorter than 240 nm was cut off by an UG11 filter (Schott-Mainz). Although POMEYC can be polymerized both in the fluid and the solid phases, this process was performed well above the lipid chain melting transition in all cases.

At low POMEYC concentrations (≤ 20 mol %) the progress of polymerization could only be followed by measurement of the lateral diffusion coefficient (cf. Figure 7). However, at higher concentrations (more than 30% POMEYC) the polymerization leads to the formation of protrusions at the vesicle surface, which assume a cauliflower-like surface profile (cf. Figure 1b).

The lipid in suspensions of small vesicles were polymerized chemically using the water-soluble AIBN (4,4-azobis(4-cyanopentanoic acid)) as initiator. The sample was heated for 1 h to 80 °C and stirred with a magnetic stirrer. This incubation time corresponded to the half-time of thermal initiator decomposition. The initiator concentration was 0.125 mg/mL at a total lipid concentration of 0.25 mg/mL. Such a high molar ratio of initiator to lipid (~ 10) was necessary since the weight fraction of lipid with respect to water is very low ($\sim 10^{-4}$). At lower initiator concentrations no appreciable polymerization was observed at 80 °C since the encounter rate of the initiator with the vesicle was too small.

(v) Lateral Diffusion Measurements. The photobleaching experiments were performed with an instrument built around a Zeiss Axiomat microscope, which was described previously.² In order to perform measurements on vesicles, the spot bleach technique was applied. Since the fluorescence recovery curves could be described to a good approximation in terms of a single diffusion species, values of the diffusion coefficients were obtained from the half-time, $\tau_{1/2}$, of fluorescence recovery. Since the intensity profile of the bleach beam (Argon Laser, 500 nm) was rectangular, the diffusion coefficient, D , is related to radius r_0 of the bleaching spot according to

$$D = 0.22r_0^2\tau_{1/2} \quad (1)$$

In all cases the bleach spot radius was $r_0 = 9 \mu\text{m}$. It should be noted that the value of D increased slightly with increasing bleach spot radius, owing to the fact that the intensity profile is not strictly rectangular. The value of D must be considered as a relative value. For the same diameter of the bleach spot, however, the values of different measurements agree to within 20%.

III. Models of Polymers and Tracers. Polymer and Tracer Motion Simulation

(i) Polymer and Tracer Models. In our models a polymer is composed of monomers, each of which is represented by a hard disk of diameter unity. "Tracers" are monomers labeled by a fluorescent marker and are not part of a polymer. A polymer model involves connecting the centers of monomers by bonds of length unity so that the monomers touch. In general, any two bonds can possess any angle with respect to each other with the proviso that the polymer can penetrate neither itself nor any other polymer. In order to attempt to identify the dominant conformations of the macrolipids, however, in the plane of the bilayer, we considered two extreme models: the collapsed polymer model (CP) and the extended polymer model (EP). A polymer in the EP model was constrained to have all its bonds collinear. The areas between the monomers were filled in to give a "stick", of constant width unity, possessing rounded ends. A polymer in the CP model was assumed to form a tightly wound spiral. It was represented by a hard disk of such a radius as to yield the same area as that of a stick possessing the same length.

In order to calculate diffusion coefficients, the following procedure was followed in setting up the model system. We did not attempt to simulate the polymerization procedure itself but assumed that this had taken place and that a steady state had been reached in which polymer bonds were neither formed nor broken. We assumed that the distribution of polymer lengths so obtained was Gaussian with an average length $\langle L \rangle$ and a width Γ . Thus, the probability that a randomly selected polymer will possess length L is

$$P(L, \langle L \rangle, \Gamma) \propto e^{-(L - \langle L \rangle)^2 / \Gamma^2} \quad (2)$$

In the interpretation that follows, we will identify $\langle L \rangle = N$, the degree of polymerization. In section IV we will discuss choices of N and Γ .

(ii) Motion Simulation Procedure. Since we have represented all of the molecules as rigid bodies, we know that their dynamics can be described by rotations around an axis perpendicular to the plane of the membrane together with a translation in that plane. In the case of the tracers and the CP model, rotations can be ignored since we have represented the molecules by hard discs. In the case of the EP model, however, we must include rotations. Accordingly, however, it is not useful to compare results for these polymer models with those obtained for other polymers where the conformational states play an important role.

Some justification is necessary in using a Monte Carlo method to simulate lateral diffusion. Although this has been addressed elsewhere,⁷ it is worthwhile reiterating the limitations of its use. This method has been used to study the self-diffusion of integral proteins in the plane of a lipid bilayer membrane in order to discover how such a diffusion coefficient depends upon the protein concentration via a hard-core protein-protein interaction and in the presence or absence of a short-range protein-protein interaction.^{7,9,11,12} Because the method involves random translations at each Monte Carlo step, the method can be used when the forces acting on the diffusing particles are predominantly random. However, one must be certain that the simulation correctly samples sufficiently well the configurations available to the system. This last proviso will lead to a correct calculation of the multiparticle distribution functions. Recently, Abney et al.,^{12b} building on the work of Ohtsuki,¹³ have shown that,

for a system of interacting particles, acted on only by random forces, the diffusion coefficient can be calculated from a knowledge of the multiparticle correlation functions. Their results are in complete agreement with those of Pink⁷ and Saxton.¹¹ This further justifies the use of the Monte Carlo method for such systems. Here, we will use the method to study the diffusion of monomeric and polymeric tracers. Polymers and tracers were distributed on an area possessing periodic boundary conditions. In each Monte Carlo step each polymer and each tracer attempted to make one move according to the recipe for its motion given below. These objects could move if in so doing they did not penetrate other objects, or themselves. The centers of the polymers either were distributed randomly and, in the EP case, oriented in a randomly chosen direction or, in high-concentration cases, were packed closely and oriented in the same direction. The polymers of different lengths were randomly intermixed. In order to initialize the system, 2000 Monte Carlo steps (i.e., 2000 Monte Carlo steps per monomer or polymer) were performed. This was followed by simulation runs of between 3000 and 5000 Monte Carlo steps in which the distance moved by each object was calculated. We found no practical differences in the results of runs for different numbers of Monte Carlo steps. When the distance moved was calculated, the periodicity of the system was ignored as described elsewhere.⁷ One such simulation, involving M_R ($M_R = 3000$ – 5000) Monte Carlo steps, defines a run. At the end of one such run we obtained the average distances moved by the tracers, r_m^2 , and the polymers, r_p^2 . A total of S such runs were carried out, and an average diffusion coefficient was calculated as

$$D_m = \frac{1}{S} \sum_{S'} r_m^2(S') / M_R$$

$$D_p = \frac{1}{S} \sum_{S'} r_p^2(S') / M_R \quad (3)$$

where $r_m^2(S')$ and $r_p^2(S')$ represent the values of those quantities obtained from run number S' . For each run we used a different initial configuration of the polymers. The number of independent cases S over which averages were computed ranged from $S = 100$ for small values of L , to $S = 163$ or $S = 189$ for longer polymers, to $S = 200$ for the largest values of L used in the CP model. In the EP model we used $S = 50$ for all cases.

(iii) Tracer Motion and Polymer Motion in the CP Model. Using a pseudorandom number generator, a direction was selected randomly from the range $(0, 2\pi)$ and a distance was selected randomly from the range $(0, d)$. We chose a value of $d = 2$ because (a) this was the maximum value for which we would avoid the problem of tracers hopping over each other and (b) it yielded an acceptance of between $\sim 20\%$ and $\sim 60\%$ of the attempts made, depending upon the concentration of polymers. It is clear that in order to associate absolute values with D_m and D_p a unit of time must be associated with each Monte Carlo step. In all cases we imposed the requirement that D_m or D_p approached unity as the polymer concentration approached zero. This then specified the time units to be associated with each Monte Carlo step. An alternative way of specifying the time unit of each Monte Carlo step would be to relate the value of the diffusion coefficient to the experimental value as the polymer concentration approaches zero. Although this was used elsewhere,⁷ we did not use it here.

(iv) Polymer Motion in the EP Model. In this case

we attempted to translate the entire polymer by a random distance in a random direction, selected as described in (iii). In addition, we selected a random angle from a range $[-\Delta\theta, \Delta\theta]$ and attempted to rotate the polymer around an axis perpendicular to the plane of the bilayer and passing through the center of the polymer. Again the magnitude of the translation was chosen from the range $(0, 2)$ for the same reason as described above. The value of $\Delta\theta$ chosen to reorient the polymer depended upon the length of the polymer. We required that the length of the arc through which the end of any polymer could move was less than or equal to 2 units as in (iii). Again this ensured that the end of a polymer would not hop over a monomer and that the attempt acceptance was between $\sim 20\%$ and $\sim 60\%$. The value of $\Delta\theta$ was thus $\Delta\theta = 2d/L = 4/L$.

(v) Kinetics Obtained by Using the Monte Carlo Method. The size of the area used was $(100)^2$ units, initialization was typically carried out for 2000 Monte Carlo steps and averaging carried out as stated above, for $M_R = 3000$ or $M_R = 5000$ Monte Carlo steps. The physical interpretation of such a simulation has been described elsewhere.⁷ Briefly, it assumes that, at the temperature of interest, the motions of the tracers and the polymers will be Brownian due to the random nature of momentum transferred from the environment in which they find themselves. If such random forces are indeed the dominant effects, then the procedure described here should yield reliable estimates of the diffusion coefficients.^{12a} The values of d used were the same for tracers and polymers. We were free to make this choice because we did not compare the diffusion coefficients of polymers and tracers. Instead we normalized polymer and tracer diffusion coefficients to unity as the polymer concentration approached zero and separately compared the polymer diffusion coefficients and the tracer diffusion coefficients at different polymer concentrations.

(vi) Fractional Area Covered by Polymers. Although monomers, whether polymerized or tracers, are represented by hard disks, the remaining components of the plane of the bilayer were represented by the remainder of the area on which the polymers and tracers were distributed. Clearly, not all this remaining area can be occupied by other molecules whose cross-sectional area is similar to that of the monomers. The effect of this is to increase the apparent concentration of polymers. This question has arisen and has been discussed in a study of protein packing in the plane of a bilayer membrane, using a model where proteins were represented by hard disks and lipids occupied the remainder of the area.⁸ In the case of two disks of different diameters greater than or equal to unity, there will be an area between them that is excluded to the tracers (disks of diameter unity), when the center-to-center distance, r , of the two disks is less than $R_1 + R_2 + 1$ where R_1 and R_2 are the radii of the two disks. The area so excluded is the average of

$$A_{\text{excl}}(R_1, R_2, r) = rh - \theta_1 R_1^2 - \theta_2 R_2^2 - \theta_0 \quad (4)$$

where

$$h = (R_2 + 1) \sin \theta_2 = (R_1 + 1) \sin \theta_1$$

$$\cos \theta_1 = [(R_1 + 1)^2 + r^2 - (R_2 + 1)^2] / 2r(R_1 + 1)$$

$$\cos \theta_2 = [(R_2 + 1)^2 + r^2 - (R_1 + 1)^2] / 2r(R_2 + 1) \quad (5)$$

We have restricted our considerations only to those cases for which $h \geq 1$. The tracers or similarly sized monomeric lipids can distort themselves in the plane of the membrane to a certain extent in order to pass between

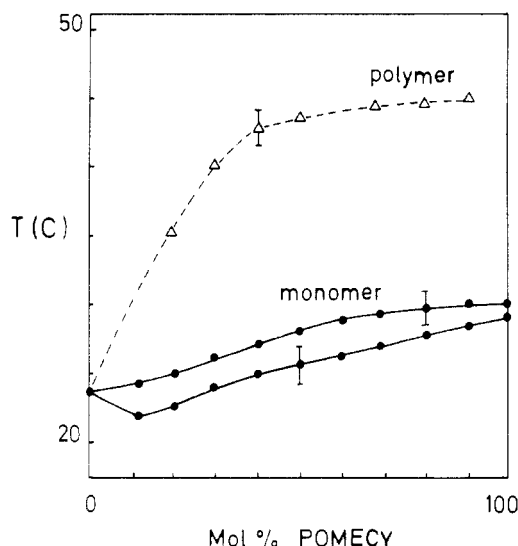


Figure 3. Phase diagram of a binary mixture of DMPC and 4,16-POMECEY before polymerization (data points marked by \bullet) and the liquidus line after chemical polymerization (\triangle). Note the nearly ideal behavior of the monomeric mixture, suggesting athermal behavior of the polymerized membranes.

the two other disks, so that we need not consider the case $h < 1$. We have computed the value of A_{excl} , averaged over a large number of Monte Carlo steps for a given distribution of polymers sizes (eq 1), for the models studied here and reduced the area occupied by that portion of the bilayer not occupied by polymers and tracers accordingly.

IV. Experimental and Theoretical Results

Phase Diagram of the Binary Mixture of DMPC with 4,16-POMECEY. The phase diagram was determined by 90° static light-scattering experiments involving a suspension of vesicles of an average diameter of about 1 μm .⁶ These were prepared by the same swelling procedure as used for the giant vesicles, which was, however, performed in a glass flask of 1-mL volume. The solvent was a buffer of pH 7.4. The final lipid concentration was 1 mg/mL (corresponding to 10^{-3} M). At this low concentration thin-walled vesicles were obtained by agitation of the flask and cooling at least once below the lipid phase transition. The latter procedure led to the splitting off of outer shells from residual multilamellar vesicles.

The static light-scattering technique has been described in detail previously.⁶ It provides an easy and reliable method to detect liquidus and solidus lines of diluted vesicle suspensions by plotting the scattered light intensity as a function of the temperature.

Figure 3 shows the phase diagram (liquidus and solidus lines) of the monomeric lipid mixture and the liquidus line after chemical polymerization for 2 h. The solidus of the latter could not be determined. The most remarkable features are the following:

(1) The rather narrow cigarlike phase diagram of the monomeric mixture provides evidence that the two components form an nearly ideal mixture.

(2) After polymerization the liquidus line increases steeply with increasing temperature below 40% of polymerizable lipid whereas a saturation point is reached at 40 mol %. This break in the liquidus line can be explained in terms of a crossover from a dilute to a semidilute two-dimensional macromolecular solution. The nearly horizontal liquidus line above 40 mol % suggests that the polymerization is not complete at high polymer concen-

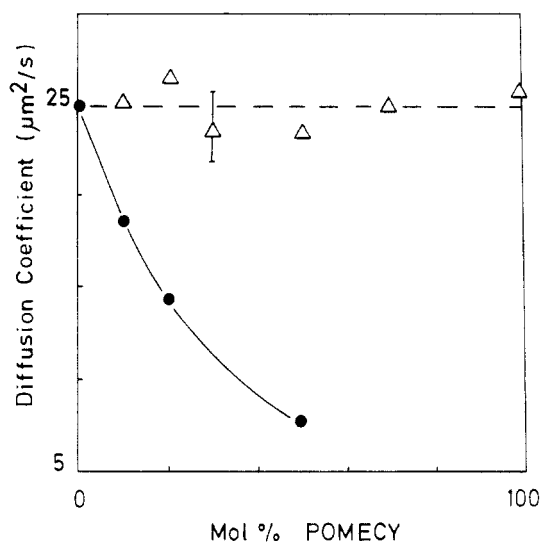


Figure 4. Lateral diffusion coefficient of monomeric fluorescent probes (diO-C₁₈) in a mixture of DMPC and 4,16-POMECEY as a function of percentage of the latter component: (\triangle) before polymerization; (\bullet) after 100 s of polymerization by UV light. Measuring temperature 50 °C. The fluorescence recovery was 80% both before and after polymerization.

trations since the lifetime of the radicals at the growing ends of the chains is then less than the encounter with a polymerizable monomer. This incompleteness of the polymerization is well-known from classical polymer science¹⁴ and has been observed in computer simulations of the process (Pink, unpublished results).

It should also be noted that separate density measurements provided evidence for a eutectic point at 20 mol % 4,10-POMECEY.

Diffusion of Monomeric and Polymerized Probe in Giant Vesicles. Figure 4 shows the variation of the diffusion coefficient of a monomeric tracer molecule in giant DMPC-POMECEY vesicles as a function of the molar fraction of polymerizable component (measured at 50 °C). The latter was photopolymerized for 100 s. Longer irradiation did not result in further polymerization. Above 50 mol % POMECEY the giant vesicles decayed rapidly into small ones ($\sim 1\text{-}\mu\text{m}$ diameter) and D_m could not be measured. The recovery was about 85% in all cases. The diffusion coefficient in the nonpolymerized vesicle was $D = 25 \mu\text{m}^2 \text{s}^{-1}$ for all compositions.

Figure 5 shows the corresponding measurement for a polymerized tracer molecule. For this experiment 1% of the fluorescent polymerizable amphiphile **1b** was added. A remarkable result is that for a given mixture the diffusion coefficient, D_p , of the macrolipid is only slightly smaller than that of the monomeric tracer. The fluorescence recovery was in all cases 85%.

Diffusion Measurements in Supported Bilayers. Three types of bilayers were prepared. The proximal layer was of DMPC in all cases and was deposited at a lateral pressure of 27 mN m⁻¹ and at 12 °C. The top (=distal) monolayer was composed of (1) DMPC, (2) mixtures of DMPC with monomeric 4,16-POMECEY, and (3) mixtures of DMPC with the polymerized lipid.

Mixed monolayers with chemically polymerized POMECEY were prepared as follows: Vesicle suspensions of the desired composition were prepared as described above. These were then polymerized chemically by addition of the initiator (AIBN) as described above. In order to remove salt and any residual initiator, the vesicle suspension was subsequently dialyzed for 12 h against pure water and then freeze-dried. Small aliquots of this powder were resolved in 3:1 CHCl₃/MeOH mixtures, and resid-

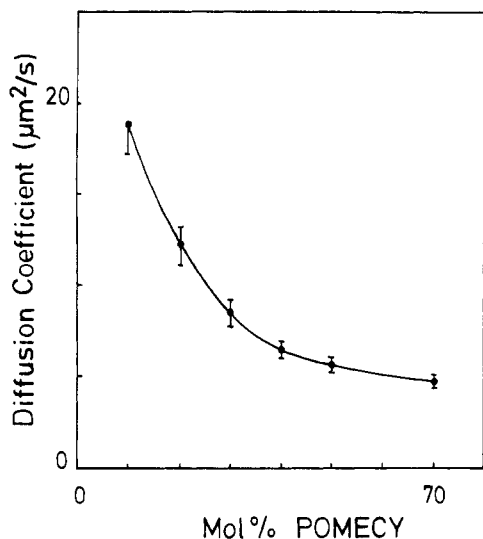


Figure 5. Lateral diffusion coefficient of a polymerized fluorescent probe in DMPC/POMEYC mixture as a function of the polymerizable lipid concentration. Measurement at 50 °C. A total of 1% of the fluorescent polymerizable amphiphile 1b was added. The fluorescence recovery was 80% in all cases.

ual nonresolved particles were removed by centrifugation. Monolayers formed spontaneously after spreading of the polymer solution on water. They were transferred onto the DMPC covered glass plates at a pressure of 17 mM m⁻¹ and 21 °C. Macromolecular tracers were incorporated into the distal monolayer by the addition of 1–3% of the polymerizable fluorescence label (1b) to the vesicle preparation prior to the polymerization. The monomeric tracer was added to the spreading solution.

The diffusion measurements were performed at 50 °C where all monolayers were certainly in the fluid state. The pertinent results are as follows:

(1) The diffusion coefficients of the NBD-DPPE probe in pure DMPC and in all mixtures with monomeric POMEYC were identical: $D_m = 18 \mu\text{m}^2 \text{s}^{-1}$. The slightly smaller value as found for DMPC bilayers is probably due to different experimental conditions.

(2) The value of D_m for the monomeric tracer NBD-DPPE in a mixture of 30% polymerized POMEYC in DMPC was $D_m = 9 \mu\text{m}^2 \text{s}^{-1}$ and was thus about 25% smaller than in the vesicle where $D_m = 12 \mu\text{m}^2 \text{s}^{-1}$.

(3) The diffusion coefficient of the probes incorporated into polymerized lipids is about 2 orders of magnitude smaller than that of the monomeric tracers. Thus for 10% polymerized POMEYC one obtains $D_p \approx 0.06 \mu\text{m}^2 \text{s}^{-1}$. Since such low values of D_p are hard to measure, this value is only an estimate. A measurement at 30% polymerized lipid yielded $D_p \approx 0.05 \mu\text{m}^2 \text{s}^{-1}$.

V. Discussion

1. Estimation of Hydrodynamic Radius of Macrolipid from Diffusion Measurements in Supported Bilayers. In a recent theoretical and experimental study^{3,5} it was shown that diffusion measurements in supported bilayers permit the determination of the coefficients of friction between opposing monolayers and/or the size of diffusing particles. This is possible provided that the external frictional drag on the membrane is determined by the friction exerted by the substrate, which is separated from the adjacent monolayer by a some nanometer-thickness of water film.⁵ The diffusion coefficient may be expressed in terms of a dimensionless param-

eter ϵ

$$\epsilon = a(\mu_w/\mu_m h_w h_m)^{1/2} \quad (6)$$

where μ_w is the viscosity of the aqueous phase, μ_m , that of the bilayer, h_w , the thickness of the water film between substrate and proximal monolayer, h_m , the membrane thickness, and a , the radius of the diffusing particle. Note that $\mu_m h_m$ is the two-dimensional viscosity of the bilayer (in Newton seconds per meter squared). The diffusion coefficient is given by

$$D = \frac{kT}{4\pi\mu_m h_m} \left(1/4\epsilon + \frac{\epsilon K_1(\epsilon)}{K_0(\epsilon)} \right)^{-1} \quad (7)$$

where K_1 and K_0 are modified Bessel functions. For $\epsilon \ll 1$ the classical Saffman–Delbruck relationship^{15,16} holds, whereas for $\epsilon \gg 1$ one is in a regime where D depends very strongly on ϵ ($D \propto \epsilon^{-2}$) and thus on the radius a .

In case of the monomeric and polymerized membrane one is in the regime $\epsilon \ll 1$ both for the monomeric and macromolecular probe as shown by the following estimate. For fluid DMPC bilayers we found previously⁵ that $\mu_m h_m \approx 1.5 \times 10^{-10} \text{ N s/m}^2$, and one obtains values of $\epsilon_m = 0.009$ for the monomeric probe ($D_m = 12 \mu\text{m}^2/\text{s}$) and $\epsilon_p = 0.06$ for the polymerized probe ($D_p \approx 7.5 \mu\text{m}^2/\text{s}$) for the case of a mixture of 30% polymerized lipid (cf. Figures 5 and 6).

With the above values of ϵ we obtain, for the ratio of the radii of the macromolecular (a_p) to the monomeric probe (a_m), $a_p/a_m \approx \epsilon_p/\epsilon_m \approx 7$. The value of $\mu_m h_m$ is expected to be higher for the polymerized membrane than for DMPC, but the above ratio depends only weakly on this parameter.

In the case of the supported bilayer the diffusion coefficient of the macromolecular species ($D_p = 0.06 \mu\text{m}^2/\text{s}$) is lower than that of the monomeric tracer by a factor of about 100 ($D_m = 9 \mu\text{m}^2/\text{s}$). This strong reduction of the diffusion coefficient is due to the fact that one is in a regime $\epsilon \approx 1$ where the friction exerted by the substrate becomes essential. The ratio of the radii of the two species can again be obtained with the help of eq 7. For the same value of the membrane viscosity as used above ($\mu_m h_m = 1.5 \times 10^{-7} \text{ erg s/cm}^2$), one obtains $a_p/a_m \approx 70$. We thus find a 1 order of magnitude difference between the hydrodynamic radii of the macrolipids in the vesicle and in the supported bilayer. This difference is attributed to the fact that the chemical polymerization procedure by which the lipids for the supported bilayer experiments were prepared yields much higher degrees of polymerization than the photochemical process. Unfortunately vesicle suspensions cannot be polymerized photochemically in order to test this hypothesis since the long exposure times required lead to substantial photodecomposition. However, further evidence for the larger coil radii of the chemically polymerized species comes from separate electron microscopy studies by the charge decoration technique¹⁶ where we found two-dimensional precipitates with minimal diameters of 100 μm in agreement with the FRAP measurements. Moreover, preliminary small-angle neutron-scattering studies (Mortensen, K.; Knoll, W.; Sackmann, E., unpublished) provide further evidence for radii of the macrolipids of some 100 μm .

The degrees of polymerization, N , derived from the above values of a_p depend on the model assumed for the coil configuration. For tightly coiled chains in two dimensions one would obtain $N \approx 50$ for the photochemically and $N \approx 6 \times 10^3$ for the chemically polymerized species. However, the chains are expected to be strongly swollen

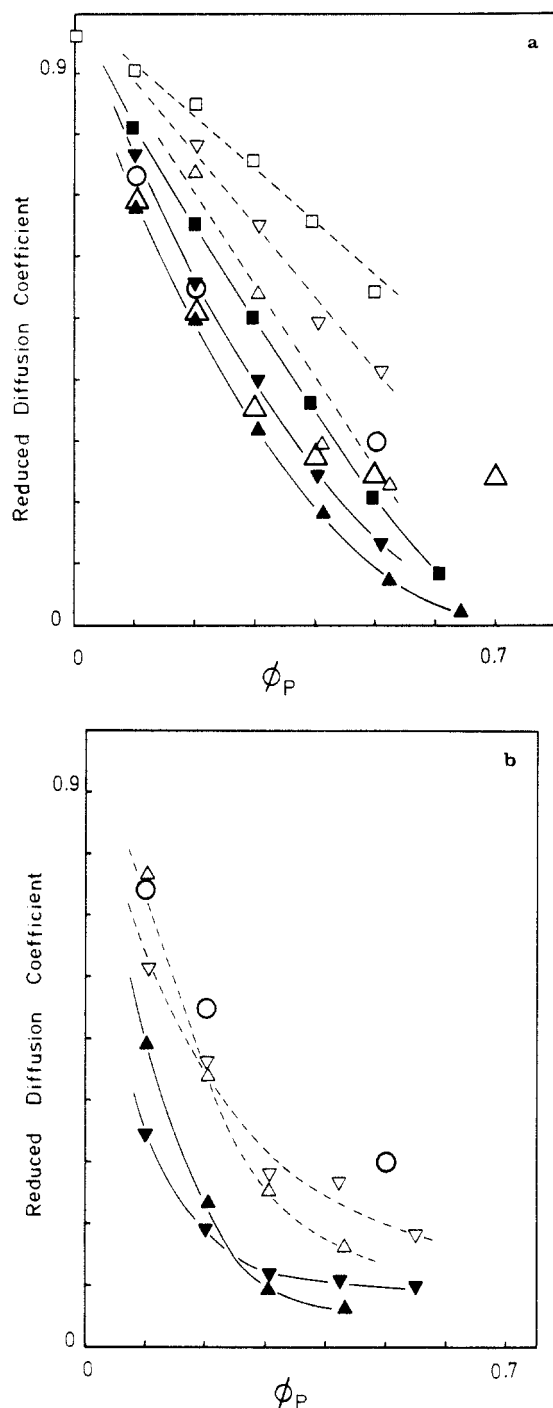


Figure 6. Comparison of measured and simulated diffusion coefficients of monomeric and polymerized tracers in mixtures of monomeric and polymerized lipid as a function of the fraction of area, ϕ_P , covered by the macrolipid: (a) Case of densely coiled-up chains (CP model) of different average degrees of polymerization, N : (Δ , \blacktriangle) $N = 8$; (∇ , \blacktriangledown) $N = 24$; (\square , \blacksquare) $N = 80$. The points indicate the actually simulated values. Dashed lines and open symbols indicate monomers; solid lines and filled symbols denote macromolecules. The large symbols give the experimental values normalized with respect to the D value in the unpolymerized membrane; (O) for monomeric tracers; (Δ) for polymers. (b) Case of straight chains (EP model). Simulations are presented for two degrees of polymerization: $N = 8$ (Δ , \blacktriangle) and $N = 24$ (∇ , \blacktriangledown). Drawn lines and filled symbols indicate macromolecules; dashed lines and open symbols show diffusion of monomeric tracer. Large open symbols (O) indicate experimental monomeric tracer results, as in (a).

for two reasons. First, the backbone of the macrolipid is rather rigid since each head group is cross-linked with two neighbors. Second, the monomers are negatively

charged and the Coulomb repulsion is expected to stretch the chains.

By using the scaling laws for 2D self-avoiding random walks for which

$$\langle a_p^2 \rangle \cong N^{3/2} a_m^2$$

one obtains $N \approx 20$ for the photochemically polymerized macrolipid and $N \approx 300$ for the chemically polymerized macrolipid.

2. Results of Simulation Studies and Comparison with Experiment. One of the primary aims of this study was to find methods for estimating the size and conformation of the macrolipids by comparison of experimental data and Monte Carlo simulation results for lateral diffusion in two dimensions.

Simulations were carried out for values of $\langle L \rangle$ equal to 8 and 24 in both models and for $\langle L \rangle = 80$ in the CP model (Figure 7). Results were obtained for values of Γ ranging from $\Gamma = 5$ to $\Gamma = 20$, and it was found that r_m^2 and r_p^2 were essentially independent of Γ . Accordingly, all runs were carried out with $\Gamma = 5$. The total number of runs, performed for a given value of $\langle L \rangle$ and fractional area covered by the polymers, was $S = 50$ in most cases. One case was studied for which we had $S = 33$. As stated above, all runs were carried out on lattices of size $(100)^2$, where each monomer was represented by a hard disk of diameter unity. Initialization to attain equilibrium was carried out for 2000 Monte Carlo steps and averaging carried out with $M_R = 3000$ steps.

Figure 6 shows the results of Monte Carlo simulations of D_m and D_p for the two models, together with experimental data for both tracers and polymers. The diffusion coefficients have all been normalized to unity at polymer concentration equal to zero. The magnitude of the confidence limits for the simulation results for tracers is indicated by the (normalized) value of D_p for $\langle L \rangle = 80$ at zero polymer concentration where the value of $D_p = 0.967$ should be unity. This difference is because, with six tracers in each of the 50 samples run, a total of 300 tracers is not sufficiently large to yield confidence limits of less than $\sim \pm 0.05$. Figure 6a shows results for the CP model with $\langle L \rangle = 8, 24$, and 80, together with experimental data for tracers and polymers. It can be seen that (i) polymer diffusion is in agreement with D_p for $\langle L \rangle = 8$ up to about 30 mol % macrolipid and that (ii) tracer diffusion is lower than D_m and exhibits a nonlinear dependence upon polymer concentration in contrast to the simulation results. Figure 6b shows simulation results for tracer diffusion. Here it is clear that neither of these results are in accord with the experimental data for tracers. The slope of the simulations is too steep for $\langle L \rangle = 8$ although there is good agreement with the value of D_m up to ~ 15 mol % macrolipid. Although the slope of the $\langle L \rangle = 24$ results is satisfactory, the numerical values are too low. The values of D_p are much lower than the results for macrolipid diffusion.

It is clear that the two models are the extreme cases of macrolipid conformation and that it is likely that the polymers exhibit a distribution of conformations that is intermediate between these two cases. In order to obtain some information about this, we considered two interpolations to intermediate cases.

(a) We assumed that, at each step, a tracer possessed a probability of taking a step characteristic of either a CP or a EP environment. Accordingly, the total distance moved, and the tracer diffusion coefficient obtained

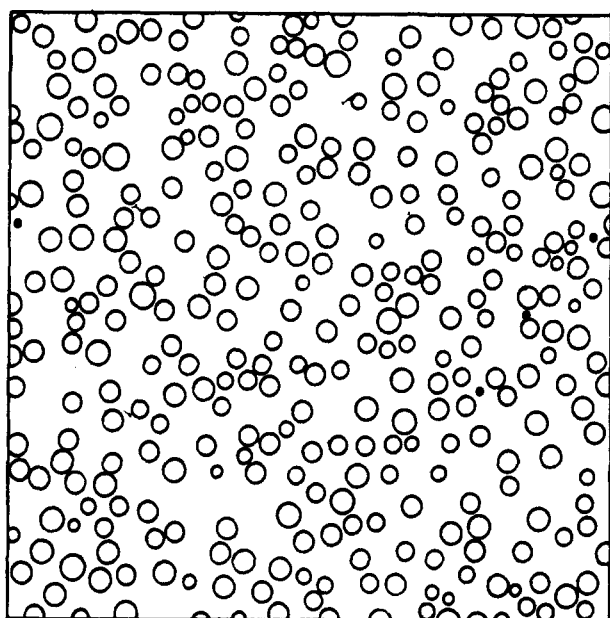
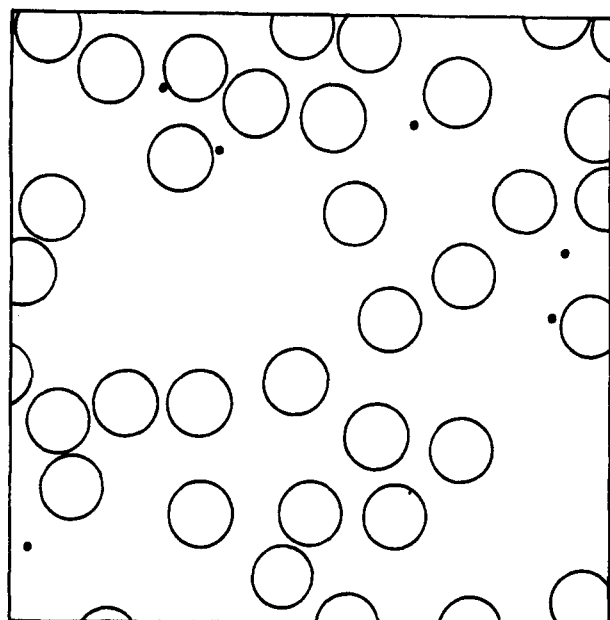


Figure 7. Instantaneous distribution of densely coiled-up macrolipids (CP model, large disks) of degrees of polymerization $N = 80$ (top) and $N = 24$ (bottom) and monomeric tracer (small filled circles) at an macromolecular area coverage of $\phi_p = 60\%$. from it, is

$$\bar{r} = \sum_i (p_C \bar{r}_{iC} + p_E \bar{r}_{iE})$$

$$D_m = p_C^2 D_m^C + p_E^2 D_m^E \quad (8)$$

where p_C and $p_E = 1 - p_C$ are the probabilities and D_m^C and D_m^E are the tracer diffusion coefficients.

(b) We assume that the diffusion coefficient is a linear combination of D_m^C and D_m^E . Here, we have $r^2 = \alpha^2 M_R$ and our assumption yields

$$\alpha^2 = p_C \alpha_C^2 + p_E \alpha_E^2$$

$$D_m = p_C D_m^C + p_E D_m^E \quad (9)$$

The approximation described in (a) is not applicable here. It assumes that in the distance moved during each step, which is characteristic of short-range diffusion, the tracer can tell what environment it is in. This is not pos-

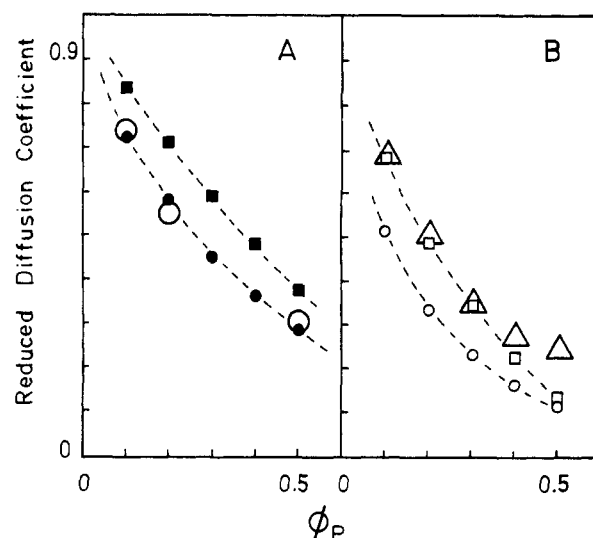


Figure 8. (A) Diffusion coefficient of monomeric tracers calculated as a linear combination of diffusion through regions of collapsed and extended polymers for $N = 24$. $p_C = 0.4$ (●) and $p_C = 0.8$ (■). Experimental measurements of monomeric tracers (○). (B) Diffusion coefficient of polymerized macrolipids calculated as a linear combination of diffusion through regions of collapsed and extended polymers for $N = 24$. $p_C = 0.4$ (○) and $p_C = 0.8$ (□). Experimental measurements of polymerized macrolipids (Δ).

sible since the scale of these two environments is larger than the step size taken by the tracer. The second approximation of (b) says that α^2 can be calculated as an average over all possible environments that the lipid diffuses through during long-range diffusion and that α^2 can be approximated by the tracer moving through the two extreme environments comprised of collapsed (C) and extended (E) polymers. In this approximation the movement of the polymer was expressed by writing α^2 as

$$\alpha^2 = p_C(p_C \alpha_{CC}^2 + p_E \alpha_{CE}^2) + p_E(p_C \alpha_{EC}^2 + p_E \alpha_{EE}^2) \quad (10)$$

where we have taken p_C (p_E) as the probability that a given polymer is diffusing through an environment of collapsed (extended) polymers, as well as the probability that the polymer is itself in a collapsed (extended) state. Equation 10 then yields

$$D_p = p_C^2 D_p^{CC} + p_C p_E (D_p^{CE} + D_p^{EC}) + p_E^2 D_p^{EE} \quad (11)$$

where $D_p^{\beta\gamma}$ is the diffusion coefficient of a polymer in a β conformation diffusing through a γ environment ($\beta, \gamma = C, E$). Although we have results for D_{CC} and D_{EE} (Figure 6), we do not have data for D_{CE} and D_{EC} . Accordingly we approximated

$$D_p^{CE} \approx D_p^{EC} \approx (D_p^{CC} + D_p^{EE})/2 \quad (12)$$

We found that neither $\langle L \rangle = 8$ nor $\langle L \rangle = 80$ gave as good a fit to the data as $\langle L \rangle = 24$, and we present results only for this case. Figure 8 shows D_m and D_p calculated for $\langle L \rangle = 24$ and two choices of p_C and compared to the experimental results. It can be seen that the choice of $p_C = 0.4$ yields a result in very good agreement with the data for D_m but that D_p lies below the experimental values by a factor of between ~ 0.6 and ~ 0.76 up to 40 mol % macrolipid. If we choose $p_C = 0.8$, however, we obtain good agreement between D_p and the data, up to ~ 35 mol %, but in the case of the monomers, D_m lies higher than the data by a factor lying between ~ 1.13 and ~ 1.29 . The curve of D_m in this case does not appear to have the correct qualitative shape, while that of D_p for the case of $p_C = 0.4$ appears to reflect the curvature of the data

reasonable well. Thus, identifying $\langle L \rangle$ with the degree of polymerization N and notwithstanding the low value of D_p obtained from the simulations, we conclude that the photopolymerized macrolipids have an average length of ~ 24 monomers and that they have a probability of being in a coiled conformation of ~ 0.4 and a probability of being in an extended conformation of ~ 0.6 .

This result agrees very well with the value of $N = 20$ –50 obtained from the diffusion coefficient of photochemically polymerized lipids in giant vesicles. It provides further evidence for our conclusion that the chemical polymerization procedure yields larger macrolipids.

Another important result that follows from Figure 8B is that the break (at $\phi_p = 0.35$) in the D_p versus ϕ_p plot of the measured diffusion coefficients of the macrolipid is not reproduced by the model. This provides further evidence for our above conclusion that the polymerization is incomplete and/or that the break corresponds to a crossover between a dilute to a semidilute regime of the two-dimensional macromolecular solution.

VI. Concluding Remarks

The present work shows that Monte Carlo simulations of the diffusion of monomeric traces and macromolecules in polymerized membranes yield valuable information on the configuration and size of the two-dimensional coils. The experimental work shows that a major problem is still the preparation of membranes with macrolipids of a defined (controlled) degree of polymerization. An important progress in this direction is the application of supported bilayers, which are separated from the substrate by thin lubricating water films. By this trick polymerized lipids may be prepared in bulk solutions and even fractionated to produce sharper molecular weight distributions. A second benefit of this technique is that the two-dimensional hydrodynamic radii of the coils can be measured, owing to the breakdown of the two-dimensional diffusion resulting in a strong (that is, nonlogarithmic) size dependence of the diffusion coefficient.

The Monte Carlo simulations studied the diffusion of monomers and macrolipids, for two extreme models. These models represented the macrolipids either as collapsed polymers or as extended polymers. It was found that the measurements are best described by a model for which the probability of a polymer being in a collapsed state is about 0.4. The agreement, within a factor of ~ 0.6 to ~ 0.75 in the cases of macrolipid diffusion and almost

exactly in the cases of monomer diffusion for a wide range of fractional area covered by the polymers, was encouraging.

We are undertaking further studies to understand the phase diagram of the photopolymerized system, as well as more detailed work to study monomer diffusion in polymers that can assume a variety of conformations. Such simulations would have been inappropriate for a first study as described here.

Acknowledgment. E.S. was James Professor in 1989 at St. Francis Xavier University and takes pleasure in thanking the Physics Department for its hospitality.

This work was supported in part by the DFG (SFB128) (E.S.) and NSERC of Canada (D.A.P.). Financial support by the Fonds der Chemische Industrie is gratefully acknowledged.

References and Notes

- (1) (a) Johnston, D. S.; Chapman, D. *Biochemistry* **1983**, *22*, 3194. (b) Ringsdorf, H.; Schlarb, F.; Venzmer, J. *Angew. Chem.* **1988**, *27*, 113.
- (2) Sackmann, E.; Eggl, P.; Fahn, C.; Bader, H.; Ringsdorf, H.; Schollmeier, M. *Ber. Bunsen-Ges. Phys. Chem.* **1985**, *89*, 1198.
- (3) Evans, E.; Sackmann, E. *J. Fluid Mech.* **1988**, *149*, 553.
- (4) McConnell, H. M.; Tamm, L. K. *Biophys. J.* **1985**, *47*, 105.
- (5) Merkel, R.; Evans, E. A.; Sackmann, E. *J. Phys. (Les Ulis, Fr.)* **1989**, *50*, 1535.
- (6) Gaub, H.; Buschl, R.; Ringsdorf, H.; Sackmann, E. *Biophys. J.* **1984**, *45*, 725.
- (7) Pink, D. A. *Biochim. Biophys. Acta* **1985**, *818*, 200.
- (8) Pink, D. A. In *Molecular Description of Biological Membrane Components by Computer Aided Conformational Analysis*; Brasseur, R., Ed.; CRC Press: Boca Raton, FL, 1989.
- (9) Pink, D. A.; Laidlaw, D. J.; Chisholm, D. *Biochim. Biophys. Acta* **1986**, *863*, 9.
- (10) (a) de Gennes, P.-G. *Scaling Concepts in Polymer Physics*; Cornell University: Ithaca, NY, 1983. (b) Baumgartner, A. In *Applications of the Monte Carlo Method in Statistical Physics*; Binder, K., Ed.; Springer-Verlag: Heidelberg, FRG, 1984.
- (11) Saxton, M. J. *Biophys. J.* **1987**, *52*, 989.
- (12) (a) Scalettar, B. A.; Abney, J. R.; Owicki, J. C. *Proc. Natl. Acad. Sci. U.S.A.* **1988**, *856*, 726. (b) Abney, J. R.; Scalettar, B. A.; Owicki, J. C. *Biophys. J.* **1989**, *55*, 817.
- (13) Ohtsuki, T. *Physica* **1982**, *110A*, 606.
- (14) Bowden, M. J. In *Macromolecules: An Introduction to Polymer Science*; Bovey, F. A., Winslow, F. H., Eds.; Academic Press: New York, 1979.
- (15) Saffmann, P. G.; Delbruck, M. *Proc. Natl. Acad. Sci. U.S.A.* **1975**, *72*, 377.
- (16) Eggl, P. Doctoral Thesis, Technical University of Munich, Munich, 1988.